

Highlights

Climate Aware Deep Neural Networks (CADNN) for Wind Power Simulation

Ali Forootani*, Danial Esmaili Aliabadi, Daniela Thrän

- Climate data-driven DNNs boost wind power forecasting accuracy
- LSTM and Transformer models excel in climate-aware wind simulations.

Climate Aware Deep Neural Networks (CADNN) for Wind Power Simulation

Ali Forootani^{*a}, Danial Esmaeili Aliabadi^a, Daniela Thrän^{a,b,c}

^a*Helmholtz Centre for Environmental Research - UFZ, Permoserstraße 15, 04318 Leipzig, Germany*

^b*DBFZ Deutsches Biomasseforschungszentrum gGmbH, Torgauer Strasse 116, 04347 Leipzig, Germany*

^c*University Leipzig, Institute for Infrastructure and Resources Management, Grimmaische Str. 12, 04109 Leipzig, Germany*

Abstract

Wind power forecasting plays a critical role in modern energy systems, facilitating the integration of renewable energy sources into the power grid. Accurate prediction of wind energy output is essential for managing the inherent intermittency of wind power, optimizing energy dispatch, and ensuring grid stability. This paper proposes the use of Deep Neural Network (DNN)-based predictive models that leverage climate datasets, including wind speed, atmospheric pressure, temperature, and other meteorological variables, to improve the accuracy of wind power simulations.

In particular, we focus on the Coupled Model Intercomparison Project (CMIP) datasets, which provide climate projections, as inputs for training the DNN models. These models aim to capture the complex nonlinear relationships between the CMIP-based climate data and actual wind power generation at wind farms located in Germany. Our study compares various DNN architectures, specifically Multilayer Perceptron (MLP), Long Short-Term Memory (LSTM) networks, and **Transformer**-enhanced LSTM models, to identify the best configuration among these architectures for climate-aware wind power simulation.

The implementation of this framework involves the development of a

^{*}Corresponding author

Email addresses: ali.forootani@ufz.de/aliforootani@ieee.org (Ali Forootani^{*}), daniel.esmaeili@ufz.de (Danial Esmaeili Aliabadi), daniela.thraen@ufz.de (Daniela Thrän)

Python package (CADNN) designed to support multiple tasks, including statistical analysis of the climate data, data visualization, preprocessing, DNN training, and performance evaluation. We demonstrate that the DNN models, when integrated with climate data, significantly enhance forecasting accuracy. This climate-aware approach offers a deeper understanding of the time-dependent climate patterns that influence wind power generation, providing more accurate predictions and making it adaptable to other geographical regions.

Keywords: Coupled Model Intercomparison Project (CMIP), Deep Neural Network (DNN), Wind Power, Climate Dataset, Long Short Term Memory (LSTM)-DNN, .

1. Introduction

The role of renewable energy (RE) in reducing greenhouse gas (GHG) emissions is crucial, which is essential for mitigating the impact of climate change. Europe’s 2030 Climate and Energy Strategy aims to reduce GHG emissions by 40% compared to 1990 levels and achieve a 27% share of renewable energy in total electricity consumption by 2030 Oberthür [1]. Wind power is one of the leading renewable energy source in terms of installed capacity and growth, contributing 15% of the European Union’s electricity consumption in 2019 Asiaban et al. [2], Zhang et al. [3]. However, wind power is highly sensitive to climate change, as future changes in wind patterns can significantly impact electricity production due to the cubic relationship between wind speed and energy potential Carvalho et al. [4]. Wind farms typically have lifetimes of 20–30 years, making it essential to estimate future changes in wind resources under climate change scenarios. Factors, such as mean wind speeds and inter-annual variability, can affect the reliability and profitability of wind energyCarvalho et al. [5], Pryor and Barthelmie [6].

Global Climate Models (GCMs), particularly from the Coupled Model Intercomparison Project (CMIP), provide crucial data for assessing climate change impacts Ahmadalipour et al. [7]. CMIP is a collaborative framework designed to compare and improve climate models by coordinating experiments across multiple research institutions Eyring et al. [8]. The project has become a cornerstone in climate science, offering standardized simulations that help evaluate models’ performance and project future climate scenarios. CMIP involves numerous coupled models that simulate interactions between different Earth system components, such as the atmosphere, oceans, land

surface, and sea ice, enabling the study of feedbacks and interactions driving climate change Lovato et al. [9]. Each CMIP phase builds on the previous one: CMIP3 supported the IPCC Fourth Assessment Report (AR4) in 2007, CMIP5 contributed to the Fifth Assessment Report (AR5) in 2013, and CMIP6, the latest phase, was used for the IPCC Sixth Assessment Report (AR6) with a more comprehensive scope, including new model components, higher resolution, and complex interactions between human activities and climate Eyring et al. [8].

Studies using CMIP5 data generally show an increase in wind resources in northern Europe and a decrease in southern Europe, with increased seasonality but inconclusive evidence for inter-annual variability Reyers et al. [10]. Recent reviews and studies have analyzed climate change impacts on wind energy using CMIP and CORDEX data, indicating a decrease in offshore wind energy resources for Europe, except in northern Europe and parts of the Iberian Peninsula deCastro et al. [11], Santos et al. [12], Costoya et al. [13]. Similar studies for the US, China, and Africa reveal region-specific changes, with projected decreases for many coastal areas and some increases in inland or specific offshore regions Chen [14], Costoya et al. [15, 16]. For instance, the Guinea coast of West Africa is expected to see a rise in wind energy resources, while the Sahel region may experience a decrease Akin-sanola et al. [17]. To make matters more complicated, the arrangement of wind farms can reduce the capacity factor of its downwind turbines and neighboring downwind farms by 20% Akhtar et al. [18].

The methodologies used in these studies involve multi-model ensembles (MMEs) validated with reanalysis data, such as ERA5, to ensure accuracy Soares et al. [19]. Despite advances in resolution and agreement between models, challenges remain, particularly regarding the spatial resolution of future climate projections and their impacts on accurately predicting RE production using less computational resources. Therefore, it is essential for revisiting previous research using CMIP6 data, which incorporates more realistic future scenarios, and notes that improvements in GCMs are expected to enhance wind resource predictions for Europe and other regions Carvalho et al. [20].

2. literature review

The growing significance of wind power prediction in recent years is largely due to its applications at a commercial scale, offering a clean alter-

native to conventional energy sources. Early work in Brown et al. [21] introduced time-series forecasting for wind power. Since then, various researchers have proposed regression-based methods for more efficient wind power prediction. For example, Liu et al. [22] presented a short-term wind power forecasting system that incorporates wavelet transforms, turbine attributes, and Support Vector Machines (SVM). The authors introduced a technique that combines data mining and K-means clustering to analyze wind power data, removing redundant data before forecasting using an Artificial Neural Network (ANN).

Yuan et al. [23] proposed a hybrid approach, where the parameters of a Least Square Support Vector Machine (LSSVM) are optimized using Gravitational Search Algorithms (GSA). Lee and Baldick [24] offered another short-term forecasting approach, training 52 ANNs and five Gaussian sub-models in parallel using historical data. These models generate power forecasts for the same time period, and a final prediction is made by aggregating their outputs. Pinson et al. [25] suggested a method based on ensemble predictions, while De Giorgi et al. [26] trained models using real wind farm data from three turbines, utilizing multiple models, including Auto regression moving average (ARMA), ANNs, and Adaptive Neuro-Fuzzy Inference Systems.

Bhaskar and Singh [27] developed an efficient wind power prediction system comprising two phases: the first phase applies wavelet decomposition to wind series, and the second phase uses a neural network to transform wind speed into power. Similarly, Abedinia and Amjady [28] presented a system that uses ANN, where the optimal number of hidden neurons is determined through a heuristic method, given that ANN performance often depends on hidden layer size. Mabel and Fernandez [29] also applied ANN to predict wind power based on three years of data from seven wind farms. Chitsaz et al. [30] proposed a system that combines clonal search algorithms and wavelet neural networks during training. Grassi and Vecchio [31] introduced a unique approach using a two-layer ANN with three neurons in each hidden layer and a single output neuron to predict wind farm energy. The first layer uses a hyperbolic tangent activation function, while the second hidden layer uses a sigmoid function.

The 2012 Global Energy Forecasting Competition showcased several methods for reliable wind power prediction Hong et al. [32], in which the utilized datasets were also described. Lei et al. [33] provided another review of techniques related to wind power forecasting. Researchers have reported various hybrid approaches for wind power forecasting Bao et al. [34], Costa et al.

[35], Foley et al. [36], and a comprehensive review of hybrid techniques is presented by Tascikaraoglu and Uzunoglu [37] proposed a method based on action-dependent heuristic dynamic programming, using a radial basis function neural network (RBFNN) to predict maximum wind power. Another hybrid method, introduced by Peng et al. [38], combines statistical and physical techniques for wind power forecasting. Bao et al. [34] used Empirical Mode Decomposition (EMD) to break wind power into high- and low-frequency components, with Relevance Vector Machines (RVM) applied to forecast these frequencies. Pinson et al. [39] employed statistical methods to enhance wind power predictions by converting prediction errors into multivariate Gaussian random variables. Nielsen et al. [40] extended recent wind power prediction systems by proposing quantile regression for probabilistic forecasting.

Ensemble-based methods have also been explored in the literature for wind speed prediction. Salcedo-Sanz et al. [41] utilized a bank of ANNs, demonstrating that their approach outperformed single neural network models for wind speed prediction. Troncoso et al. [42] employed various regression trees to predict wind speeds across multiple wind farms and compared the results with those from ANNs and Support Vector Regression (SVR). Ortiz-García et al. [43] proposed an ensemble technique using a bank of SVRs to forecast wind speed, outperforming MLPs. Zhang et al. [44] presented a hybrid model for wind speed forecasting using data from northwest China. To address the limitations of ANNs in forecasting, Ma et al. [45] developed a model based on dynamic fuzzy ANNs. Despite the success of statistical and hybrid approaches, each has its own limitations Jung and Broadwater [46].

Although these models are accurate enough to address operational needs based on past data, the underlying climate system is changing, and hence, these models may not be fit anymore for future needs Esmaeili Aliabadi et al. [47]. To this end, in this manuscript, we are preparing the ground for the next generation of ANN-based models that can utilize the results of climate models.

Moreover, Previous efforts to estimate wind power generation using physics-based models were hindered by the significant variability in climate scenarios and the limitations of current climate models in providing scenario-specific data with high spatial and temporal resolution Lehneis et al. [48]. To address these challenges, we have shifted from physical simulation models to employing DNN architectures, leveraging the processed CMIP climate dataset to enhance the accuracy of wind power predictions.

2.1. Contributions

This article introduces a refined methodology for integrating CMIP6 climate data into wind energy forecasting over Germany. The proposed approach enhances key aspects such as data preparation, spatial interpolation, temporal alignment, and scaling, enabling effective localized forecasts at wind turbine sites. By tailoring CMIP6 data for machine learning applications, we bridge the gap between large-scale climate models and localized renewable energy prediction. Key Methodological Advancements are as follows:

- Data Preparation:
 - Temporal resampling and conversion to a standardized time format ensure compatibility with time-series forecasting models, particularly deep learning architectures like LSTM networks that rely on consistent temporal structures for accurate predictions.
 - Feature normalization is applied to harmonize input scales, promoting balanced contributions during model training and improving predictive performance.
- Spatial Interpolation: An interpolation algorithm accurately maps rotated pole datasets to geographic coordinates, ensuring precise spatial alignment with wind conditions across Germany—a critical step for localized forecasting.
- Model Evaluation: This study systematically evaluates multiple deep learning architectures, including Multi-Layer Perceptrons (MLPs), LSTM networks, and Transformer-enhanced LSTMs:
 - MLPs effectively capture static relationships but struggle with the temporal and non-linear dependencies inherent in climate data.
 - Transformer-enhanced LSTMs, despite their complexity, did not yield significant performance improvements, indicating a mismatch with the dataset’s characteristics.
 - LSTM networks outperform others due to their robust ability to model sequential and long-term dependencies, making them the preferred architecture for climate-driven renewable energy forecasting.

To facilitate reproducibility, we developed a dedicated Python package, CADNN, leveraging PyTorch for deep learning implementation. This package includes modules for data preparation, model training, and evaluation, optimized for large climate datasets with temporal and spatial components. By sharing this package, we provide the research community with a robust toolset for implementing DNN-based wind power simulation, fostering accessible and efficient workflows.

To the best of our knowledge, this is the first study to integrate CMIP6 climate data into localized wind power simulation at this scale. Our findings highlight LSTM networks as the most effective architecture for climate-based renewable energy prediction, offering valuable insights and establishing best practices for preparing and utilizing climate data in machine learning applications.

This paper is organized as follows: In section 3 we briefly provide a background about DNN models that we make use in this article. We analyze the meteorological data in section 4 in CMIP data files over Germany in the locations of wind farms. In section 5 we investigate the performance of three DNN architectures in mapping nonlinear relationship of climate dataset and the wind power. The conclusion is given in section 6.

3. Mathematical Background of DNNs

A DNN is a type of ANN with multiple layers of neurons. The primary components of a DNN are neurons, layers, weights, and activation functions Forootani et al. [49].

Mathematical Representation. Let \mathbf{x} represent the input vector, and $\mathbf{W}_l, \mathbf{b}_l$ represent the weight matrix and bias vector of the l -th layer, respectively. The output of the l -th layer is computed as:

$$\mathbf{z}_l = \mathbf{W}_l \mathbf{a}_{l-1} + \mathbf{b}_l,$$

where \mathbf{a}_{l-1} is the activation from the previous layer. The activation function σ is applied to produce the output of the layer:

$$\mathbf{a}_l = \sigma(\mathbf{z}_l),$$

Common choices for activation functions include: (i) Sigmoid: $\sigma(x) = \frac{1}{1+e^{-x}}$; (ii) ReLU: $\sigma(x) = \max(0, x)$; (iii) Tanh: $\sigma(x) = \tanh(x)$.

The final output layer of the network computes the predicted value:

$$\mathbf{y}_{\text{pred}} = \mathbf{W}_L \mathbf{a}_{L-1} + \mathbf{b}_L,$$

Training. DNNs are typically trained using back-propagation and an optimization algorithm (usually stochastic gradient descent, SGD). The loss function $L(\mathbf{y}_{\text{pred}}, \mathbf{y}_{\text{true}})$ measures the difference between the predicted and true outputs. The goal of training is to minimize the loss by adjusting the weights and biases through gradient descent:

$$\mathbf{W}_l \leftarrow \mathbf{W}_l - \eta \frac{\partial L}{\partial \mathbf{W}_l},$$

where η is the learning rate.

3.1. LSTM Networks

LSTM networks are a type of Recurrent Neural Network (RNN) designed to address the vanishing gradient problem in traditional RNNs, particularly for sequences with long-range dependencies Huang et al. [50].

LSTM Architecture. An LSTM unit consists of several gates: input gate, forget gate, and output gate. The cell state \mathbf{C}_t and hidden state \mathbf{h}_t are updated at each time step. The gates in LSTM are computed as follows:

- Forget gate:

$$\mathbf{f}_t = \sigma(\mathbf{W}_f[\mathbf{h}_{t-1}, \mathbf{x}_t] + \mathbf{b}_f),$$

- Input gate:

$$\begin{aligned} \mathbf{i}_t &= \sigma(\mathbf{W}_i[\mathbf{h}_{t-1}, \mathbf{x}_t] + \mathbf{b}_i), \\ \tilde{\mathbf{C}}_t &= \tanh(\mathbf{W}_C[\mathbf{h}_{t-1}, \mathbf{x}_t] + \mathbf{b}_C), \end{aligned}$$

- Output gate:

$$\mathbf{o}_t = \sigma(\mathbf{W}_o[\mathbf{h}_{t-1}, \mathbf{x}_t] + \mathbf{b}_o),$$

where σ is the activation function ¹. The cell state is updated as:

$$\mathbf{C}_t = \mathbf{f}_t \odot \mathbf{C}_{t-1} + \mathbf{i}_t \odot \tilde{\mathbf{C}}_t,$$

where \odot denotes element-wise multiplication.

The hidden state is updated as:

$$\mathbf{h}_t = \mathbf{o}_t \odot \tanh(\mathbf{C}_t).$$

¹The candidate cell state ($\tilde{\mathbf{C}}_t$) and the final cell state modulation ($\tanh(\mathbf{C}_t)$) use tanh because the cell state stores the actual information (or “content”) of the memory

Training. Similar to DNNs, LSTMs are trained via backpropagation through time (BPTT), where gradients are computed for each time step and used to update the weights using an optimization algorithm like SGD or Adam.

3.2. Transformer-based DNNs

Transformer networks are primarily used for sequence-to-sequence tasks such as machine translation, and text summarization Vaswani et al. [51]. Transformer utilize self-attention mechanisms to model dependencies between elements in a sequence Forootani et al. [52].

Transformer Architecture. The Transformer model consists of an encoder and a decoder, both composed of stacked layers of self-attention and feed-forward neural networks.

Self-Attention. For each input sequence, the self-attention mechanism computes a scaled dot-product attention for each query \mathbf{q}_i , computed as:

$$\text{Attention}(\mathbf{q}_i) = \text{softmax} \left(\frac{\mathbf{q}_i \mathbf{k}_j^T}{\sqrt{d_k}} \right) \mathbf{v}_j,$$

where \mathbf{q}_i is the query vector for the i -th element, \mathbf{k}_j is the key vector for the j -th element, \mathbf{v}_j is the value vector for the j -th element, and d_k is the dimension of the key vector.

The self-attention mechanism captures dependencies by weighting the importance of each element in the sequence with respect to others.

Multi-Head Attention. The model applies multiple attention mechanisms in parallel (multi-head attention) to capture different aspects of dependencies.

Position Encoding. Since Transformers do not have an inherent notion of sequence order, position encodings are added to the input to provide information about the position of tokens in the sequence. The position encoding \mathbf{p}_t for position t is typically computed as:

$$\mathbf{p}_t = \left[\sin\left(\frac{t}{10000^{\frac{2i}{d}}}\right), \cos\left(\frac{t}{10000^{\frac{2i+1}{d}}}\right) \right] \quad \text{for } i = 1, 2, \dots, d,$$

where d is the dimension of the input.

Feed-Forward Network. After the attention mechanism, the output is passed through a feed-forward neural network:

$$\mathbf{y}_i = \text{ReLU}(\mathbf{W}_2(\text{ReLU}(\mathbf{W}_1\mathbf{x}_i + \mathbf{b}_1)) + \mathbf{b}_2),$$

Training. Transformer are trained using maximum likelihood estimation and the cross-entropy loss function, with optimization algorithms like Adam.

Summary of Key Differences for different DNN structures are as follows:

- **MLPs:** General-purpose neural networks that model complex relationships via multiple layers of neurons and nonlinear activation functions.
- **LSTMs:** A type of RNN designed to handle long-range dependencies in sequential data using gating mechanisms to manage memory over time.
- **Transformers:** Sequence models based on self-attention mechanisms that capture long-range dependencies more effectively than RNN s and LSTMs, especially in tasks like machine translation.

4. Analysis of Meteorological Data Over Germany

Effective data processing techniques are crucial for managing and analyzing large-scale datasets in scientific and industrial domains, particularly in renewable energy and climate studies. Techniques such as data cleaning, validation, interpolation, and machine learning integration are essential for extracting actionable insights from atmospheric and geospatial data, including wind speed, pressure, and temperature. Publicly accessible datasets like those from CMIP6 require spatial interpolation to estimate values at specific locations, using methods like the *Regular Grid Interpolator* for geographic grids Jung and Broadwater [46], Weiser and Zarantonello [53], and temporal interpolation to handle missing time-series data. Climate models often provide results with a lower temporal resolution (typically a 3-hour resolution²), while wind power data is recorded hourly or even quarter-hourly (e.g., Open Power System Data³). To align these datasets, a resampling and aggregation approach is necessary, transforming wind power and pressure data into standard intervals, such as 3-hour periods, to match the climate data.

²<https://cds.climate.copernicus.eu/datasets>

³<https://open-power-system-data.org/>

In this context, accurately preparing wind speed and surface pressure datasets for any region⁴ involves extracting and processing CMIP6 data. This preparation includes spatial interpolation, scaling, and temporal resampling to ensure the data is suitable for wind power simulation models and other atmospheric analyses. To capture fine spatial variations, latitude and longitude coordinates are defined at a specific resolution, and geographical ranges relevant to the selected region (i.e., Germany in this study) are filtered. This approach streamlines the CMIP data, yielding a focused dataset that supports robust analysis of wind speed and pressure in the region, facilitating effective decision-making in renewable energy forecasting and climate studies.

In climate data analysis, especially when using rotated pole datasets such as CMIP, transforming coordinates and spatially interpolating data onto a target region (e.g., Germany) are critical for ensuring that the extracted variables accurately represent the geographical area of interest. The following two steps—coordinate transformation and spatial interpolation—are implemented to achieve this precision.

Coordinate Transformation. The CMIP datasets utilize a rotated pole coordinate system where geographic coordinates are defined relative to an artificial “rotated” pole. This coordinate system is commonly used to reduce grid distortion in regional climate modeling Grose et al. [54]. To align with standard geographic coordinates (latitude and longitude), a coordinate transformation is required. Using the Algorithm algorithm 1, we convert the standard latitude and longitude of target points within Germany to this rotated coordinate system. This ensures that each point of interest in Germany is accurately aligned with the dataset’s coordinate system before data extraction, maintaining the spatial integrity of climate variables such as wind speed.

Spatial Interpolation and Efficient Spatial Querying with KD-Tree on the climate dataset. After transforming coordinates, the next challenge is to spatially match these target points to the dataset’s grid points, which may not align perfectly. The `cKDTree` is a binary space-partitioning data structure used to organize points $\mathbf{V} = \{\mathbf{v}_1, \mathbf{v}_2, \dots, \mathbf{v}_n\} \in \mathbb{R}^k$, where each node splits the space at a median point along one of the k dimensions. At depth d , the space is split along dimension $d \bmod k$ using the median value,

⁴Germany is selected as a case study in this manuscript.

$\mathbf{v}_{\text{split}} = \text{median}(v_1^{(d \bmod k)}, \dots, v_n^{(d \bmod k)})$, dividing points into two subsets. For nearest-neighbor search, given a query point $\mathbf{q} \in \mathbb{R}^k$, it efficiently finds the closest point $\mathbf{v}_{\text{nearest}} = \arg \min_{\mathbf{v}_i \in \mathbf{V}} \|\mathbf{q} - \mathbf{v}_i\|_2$. The **KD-tree** accelerates queries like nearest neighbors or radius searches by pruning irrelevant parts of the space, reducing search complexity to $O(\log n)$ on average ⁵.

Constructing a **KD-Tree** for the grid enables rapid spatial querying, significantly reducing the computational complexity compared to exhaustive search methods. This function then performs a nearest-neighbor search, returning the closest available grid point to each transformed target coordinate. This approach minimizes interpolation errors and ensures that the extracted data points accurately represent spatial locations within the target region.

This combination of coordinate transformation and **KD-Tree** spatial querying provides an accurate and computationally efficient methodology for extracting climate variables at the desired spatial resolution. It enhances the fidelity of regional climate analysis by aligning extracted data points with geographic coordinates in a physically meaningful way.

In conclusion the **KD-Tree** algorithm is used to efficiently map the extracted wind speeds or pressure surface from the rotated grid of the CMIP6 dataset to a regular latitude-longitude grid over Germany, ensuring spatial data consistency during the extraction process. However we need another interpolation algorithm to further refine this data by interpolating the wind speeds or pressure surface onto specific, irregularly spaced target locations (e.g., measurement sites), addressing the mismatch between the extracted grid and the desired points of analysis.

Spatial Interpolation at the location of wind turbines. To refine the spatial representation of both wind speed and pressure data, interpolation techniques are applied. Wind speeds and pressure levels at the locations of wind farms are interpolated onto the desired target locations (such as wind turbine sites or measurement stations). In particular, we employ a linear interpolation method (*Regular Grid Interpolator*), which performs multivariate interpolation on a regular grid in n -dimensional space. Suppose the function $f : \mathbb{R}^n \rightarrow \mathbb{R}$ is known on a set of regularly spaced grid points $\{x_1^i, x_2^j, \dots, x_n^k\}$, where each $x_i \in X_i$ forms a regular grid for each dimension. The objective is to estimate $f(\mathbf{x})$, where $\mathbf{x} = (x_1, x_2, \dots, x_n)$, which is not necessarily a grid

⁵Here, the “cKDTree” algorithm from “scipy.spatial” is applied to efficiently locate the nearest dataset grid points for each transformed coordinate Virtanen et al. [55].

point.

To interpolate at \mathbf{x} , let $(x_1^i, x_1^{i+1}), \dots, (x_n^k, x_n^{k+1})$ be the grid intervals that contain x_1, \dots, x_n . For linear interpolation in each dimension, the value of $f(\mathbf{x})$ is obtained as a weighted combination of the function values at the corners of the grid cell surrounding \mathbf{x} . Denote the neighboring grid points as $f(x_1^i, x_2^j, \dots, x_n^k)$, and the interpolated value is given by:

$$f(\mathbf{x}) \approx \sum_{i_1=0}^1 \sum_{i_2=0}^1 \cdots \sum_{i_n=0}^1 w_{i_1 i_2 \dots i_n} f(x_1^{i_1}, x_2^{i_2}, \dots, x_n^{i_n}),$$

where $w_{i_1 i_2 \dots i_n}$ are the weights based on the relative distances between \mathbf{x} and the surrounding grid points. For example, for linear interpolation in 1-D, the interpolation formula between two grid points x_i and x_{i+1} is:

$$f(x) \approx \frac{x_{i+1} - x}{x_{i+1} - x_i} f(x_i) + \frac{x - x_i}{x_{i+1} - x_i} f(x_{i+1}).$$

In cases where interpolated values can not be computed due to a lack of surrounding data, the nearest available data points were used as a fallback, ensuring that the final interpolated dataset contained no gaps. Interpolation allows for higher spatial granularity of both wind speed and pressure data, enhancing the model’s ability to predict localized weather conditions. Algorithm 2 summarizes the interpolation method that is explained earlier.

Temporal Resampling. Wind power production usually is measured hourly⁶, however both wind speed and surface pressure in CMIP data are available in 3-hour interval, therefore the power is resampled. This approach retains essential temporal variability while reducing computational requirements for subsequent analysis. To ensure consistency across the dataset, the datetime information is standardized, facilitating time-based calculations in machine learning workflows. This transformation enables the data to be effectively utilized in time-series forecasting models, ensuring that temporal patterns are accurately captured. These steps of resampling and time standardization are crucial for preparing the data for machine learning applications, such as LSTM networks, which depend on a regular time structure to enhance forecasting accuracy in wind power prediction.

⁶<https://open-power-system-data.org/>

Data Scaling and Normalization. Data scaling is an essential step in preparing datasets for machine learning models, which can be sensitive to the range and distribution of input values. Here, wind speed and pressure data were scaled using a Min-Max scaling technique to map values between -1 and 1 . This approach ensures that each feature contributes equally to the learning process, avoiding biases from variables with larger numerical ranges.

Normalizing variables like wind speed, pressure, and time ensures that machine learning models can identify patterns effectively, without being affected by differences in scale across features. This scaling process enhances the performance of machine learning algorithms, such as DNNs, which typically perform better when input features are standardized.

4.1. Dataset Visualization

To facilitate interpretation, various visualization tools are used. In Figure 1, we present the average surface wind speed across European countries based on the CMIP dataset. We apply algorithm 1 to transform the coordinates, followed by algorithm 2 to interpolate meteorological data specifically for the locations of wind farms in Germany. Notably, the locations of these wind farms are sourced from the EE-Monitor project,⁷ which provides environmental insights into renewable energy expansion in Germany.

Wind speed and surface pressure data, each with a shape of (2928×28574) , have been extracted from the CMIP dataset. Here, 2928 represents the number of time steps at 3-hour intervals across one year, and 28574 represents the various grid points. These grid points correspond to a latitude and longitude grid with shapes (157) and (182) , respectively.

To focus on specific target locations, wind speed and pressure data are interpolated, resulting in arrays with shapes of (2928×232) for both variables. The target points, which represent the locations of wind farms in Germany, are provided as specific coordinates of interest with a shape of (232×2) . This data structure highlights the challenge of high dimensionality within climate datasets.

In Figure 2, the surface wind speed is shown at a location with coordinates Lat 49.77, Lon 10.16 correspond to the city of Würzburg in Germany for the year 2020. Also, Figure 4 visualizes spatial variations in mean wind

⁷EE Monitor provides information on the expansion of renewable energies in Germany from an environmental perspective, <https://web.app.ufz.de/ee-monitor/>.

Algorithm 1: Rotate Coordinates

Input: Latitude ϕ , Longitude λ , Pole Latitude ϕ_p , Pole Longitude λ_p (in degrees)

Output: Rotated Latitude ϕ_{rot} , Rotated Longitude λ_{rot} (in degrees)

1 **Convert coordinates to radians:**

2

$$\phi \leftarrow \frac{\pi}{180} \cdot \phi, \quad \lambda \leftarrow \frac{\pi}{180} \cdot \lambda, \quad \phi_p \leftarrow \frac{\pi}{180} \cdot \phi_p, \quad \lambda_p \leftarrow \frac{\pi}{180} \cdot \lambda_p$$

3 **Calculate longitude difference:**

4

$$\Delta\lambda \leftarrow \lambda - \lambda_p$$

5 **Compute rotated latitude:**

6

$$\phi_{rot} \leftarrow \arcsin(\sin(\phi) \cdot \sin(\phi_p) + \cos(\phi) \cdot \cos(\phi_p) \cdot \cos(\Delta\lambda))$$

7 **Compute rotated longitude:**

8 Define:

9

$$y = \cos(\phi) \cdot \sin(\Delta\lambda),$$

$$x = \sin(\phi) \cdot \cos(\phi_p) - \cos(\phi) \cdot \sin(\phi_p) \cdot \cos(\Delta\lambda)$$

10 Then calculate:

$$\lambda_{rot} \leftarrow \lambda_p + \text{atan2}(y, x)$$

where:

$$\text{atan2}(y, x) = \begin{cases} \arctan\left(\frac{y}{x}\right) + \pi & \text{if } x < 0 \text{ and } y \geq 0 \\ \arctan\left(\frac{y}{x}\right) + 2\pi & \text{if } x < 0 \text{ and } y < 0 \\ \arctan\left(\frac{y}{x}\right) & \text{if } x > 0 \\ \frac{\pi}{2} & \text{if } x = 0 \text{ and } y > 0 \\ -\frac{\pi}{2} & \text{if } x = 0 \text{ and } y < 0 \\ 0 & \text{if } x = 0 \text{ and } y = 0 \end{cases}$$

11 **Convert rotated coordinates back to degrees:**

12

$$\phi_{rot} \leftarrow \frac{180}{\pi} \cdot \phi_{rot}, \quad \lambda_{rot} \leftarrow \frac{180}{\pi} \cdot \lambda_{rot}$$

13 **return** $(\phi_{rot}, \lambda_{rot})$

Algorithm 2: Interpolation of Meteorological Data

Input: Meteorological data $\mathbf{X} \in \mathbb{R}^{T \times M \times N}$ (e.g., wind speeds or pressures), grid latitudes $\mathbf{L}_{\text{lat}} \in \mathbb{R}^M$, grid longitudes $\mathbf{L}_{\text{lon}} \in \mathbb{R}^N$, target points $\mathbf{P} \in \mathbb{R}^{P \times 2}$

Output: Interpolated meteorological values at target points $\mathbf{X}_{\text{interp}} \in \mathbb{R}^{T \times P}$

1 **Sort grid latitudes and longitudes:**

2

$$\mathbf{L}_{\text{lat}} \leftarrow \text{sort}(\mathbf{L}_{\text{lat}}), \quad \mathbf{L}_{\text{lon}} \leftarrow \text{sort}(\mathbf{L}_{\text{lon}})$$

3 **Initialize matrix for interpolated values:**

4

$$\mathbf{X}_{\text{interp}} \leftarrow \text{zeros}(T, P)$$

5 **for each target point $\mathbf{p} \in \mathbf{P}$ and each time step t do**

6 **Reshape** meteorological data \mathbf{X}_t into a 2D grid.

7 **Linear interpolation:**

8 Define:

$$\mathbf{X}_{\text{linear}}(\mathbf{p}) = \sum_{i=1}^2 \sum_{j=1}^2 w_{ij} \cdot \mathbf{X}(\mathbf{L}_{\text{lat}}[x_i], \mathbf{L}_{\text{lon}}[y_j])$$

where w_{ij} are interpolation weights, and (x_i, y_j) are indices of the grid points around \mathbf{p} .

9 **if linear interpolation fails to find values in $\mathbf{X}_{\text{linear}}$ then**

10 **Nearest-neighbor interpolation:**

11 Define:

$$\mathbf{X}_{\text{nearest}}(\mathbf{p}) = \mathbf{X}(\mathbf{L}_{\text{lat}}[x_{\text{nearest}}], \mathbf{L}_{\text{lon}}[y_{\text{nearest}}])$$

where $(x_{\text{nearest}}, y_{\text{nearest}})$ are indices of the closest grid points to \mathbf{p} .

12 **Store** interpolated values for the current time step in $\mathbf{X}_{\text{interp}}$.

13 **return** $\mathbf{X}_{\text{interp}}$

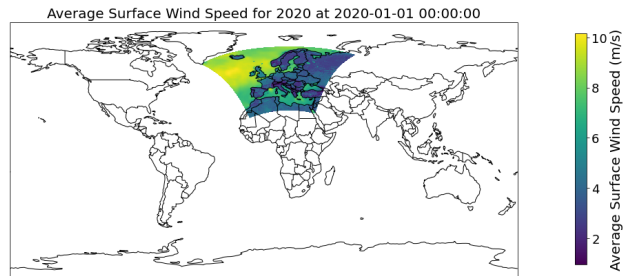


Figure 1: Average surface wind speed for Europe on 2020-01-01 at 00:00:00 from CMIP dataset.

speeds across a grid of target locations, providing a comprehensive representation of wind dynamics in Germany. Color intensity indicates average wind speed values, where areas with higher mean speeds are highlighted to aid in assessing wind power potential and regional variability over the observed period.

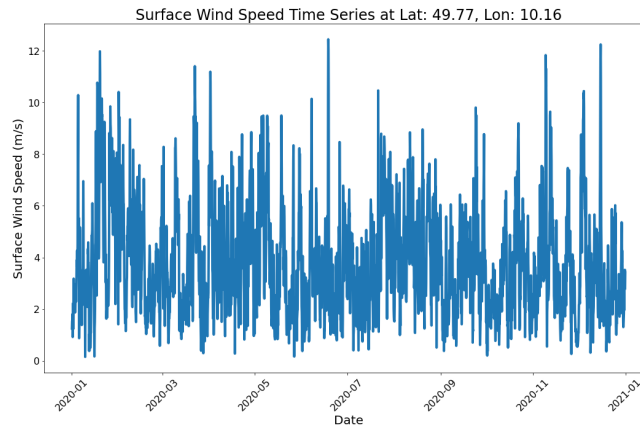


Figure 2: Surface Wind Speed for the entire year 2020 at coordinates: Lat 49.77, Lon 10.16 correspond to the city of Würzburg in Germany.

The map in Figure 3b illustrates the spatial distribution of mean atmospheric pressure across Germany, where color intensity reflects pressure levels in kilopascals (KPa). This visualization enables an analysis of regional pressure variations and trends, which are essential for understanding atmospheric conditions relevant to weather forecasting and climate studies.

The histogram in fig. 5 illustrates the distribution of wind speeds across the dataset, highlighting the frequency of various wind speed intervals. This

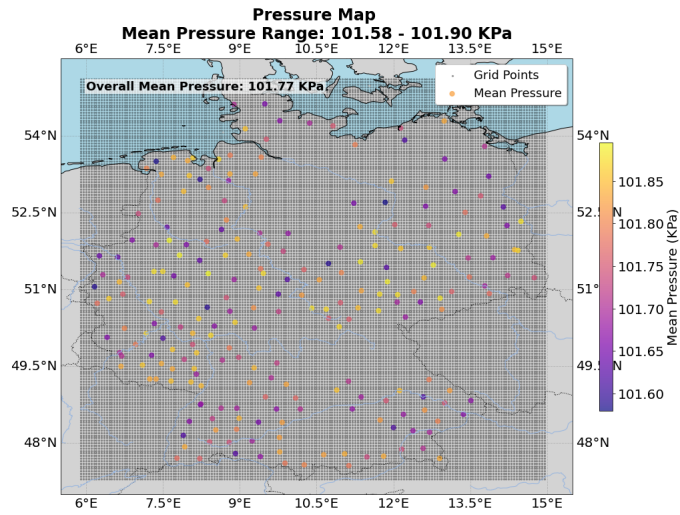
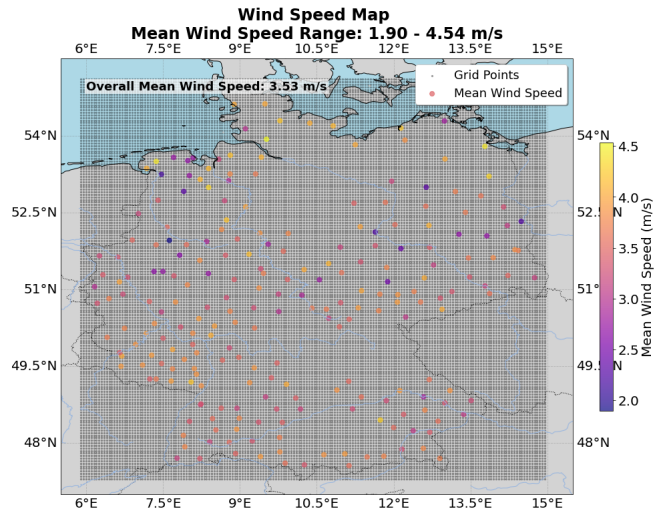


Figure 3: (a) Interpolation of wind speed over Germany computed by algorithm 1 and algorithm 2 at the locations of wind farms. (b) Interpolation of pressure surface over Germany computed by algorithm 1 and algorithm 2 at the locations of wind farms.

distribution analysis provides insight into prevalent wind conditions, essential for assessing wind energy potential and variability.

The histogram in fig. 6 displays the distribution of atmospheric pressure

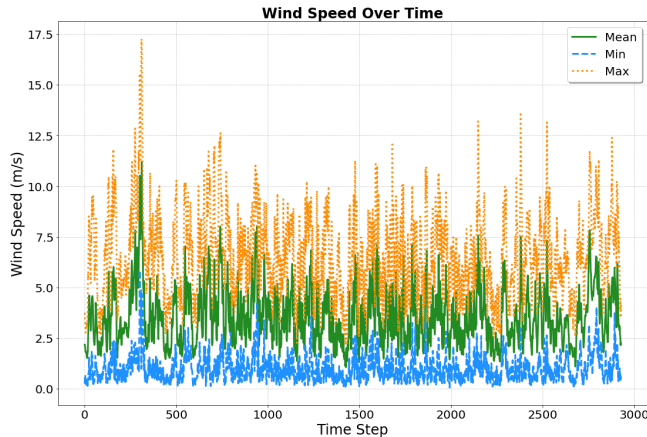


Figure 4: Wind speed with the resolution of 3 hours at locations of operational wind power plants in 2020.

values across the dataset, converted to kilopascals (KPa). This frequency analysis of pressure variations aids in understanding atmospheric patterns, which is crucial for weather prediction and climate-related studies.

5. DNNs for Wind Power Production Forecast Enhanced with Climate Data

Previous attempts to generate a high-quality estimation of wind power generation based on climate models using physics-aware models did not yield acceptable results due to the inherent variabilities of climate scenarios and the inability of current climate models to offer scenario-based data with high spatial and temporal sensitivity Lehneis et al. [48]. Thus, instead of using physical simulation models, we employ DNN architectures on the processed CMIP climate dataset to improve prediction accuracy in wind power simulating. Specifically, we compare three types of DNN models—MLPs, LSTM networks, and Transformer-enhanced LSTM networks—to evaluate their performance and suitability for this task.

Advancing wind power simulating with climate data requires machine learning models capable of capturing complex, non-linear patterns and temporal dependencies. DNNs are well-suited for this purpose, as they can adapt to a wide range of input structures and feature relationships. MLPs are particularly effective for capturing non-linear input-output mappings in high-dimensional data, making them useful for static feature extraction from cli-

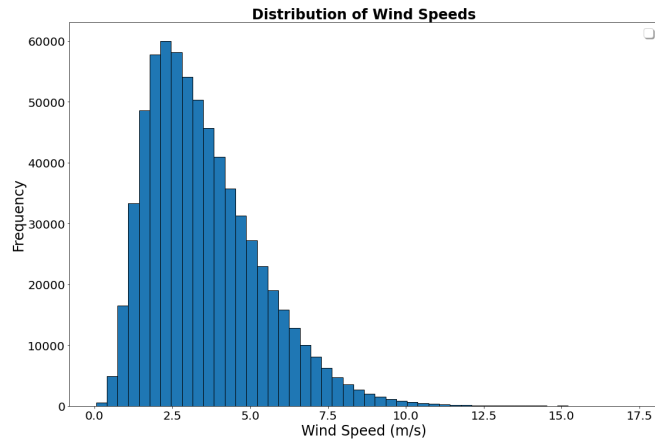


Figure 5: Distribution of wind speeds across the dataset for the year 2020.

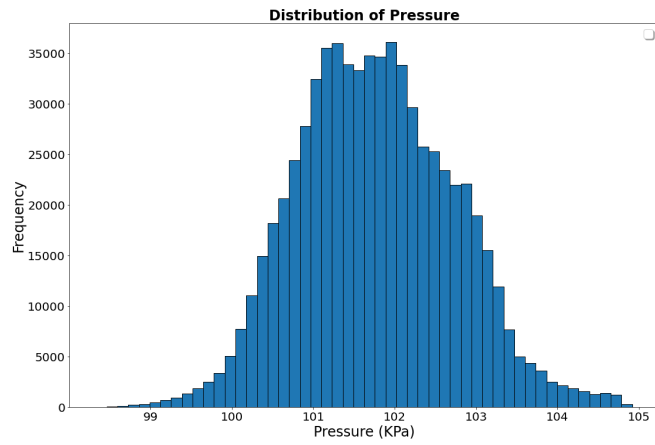


Figure 6: Distribution of pressure surface across the dataset for the year 2020.

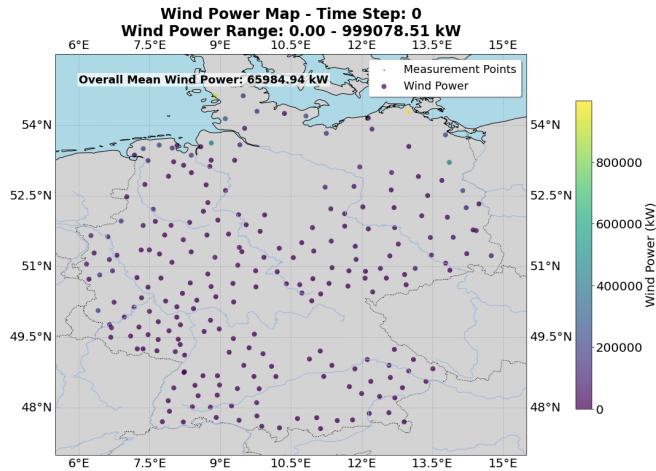


Figure 7: Wind power generation power in 2020 at time step 00:00:00, with resolution of 3 hours.

mate variables such as wind speed and surface pressure. However, as MLPs are fully connected networks without memory structures, they are less effective at modeling sequential dependencies over time. This limitation can affect their accuracy in time-sensitive forecasting applications.

In contrast, LSTM networks, a type of recurrent neural network (RNN), are designed to capture time dependencies through their unique gating mechanisms and memory cells. This structure enables them to retain information over extended periods, allowing LSTM networks to model sequential relationships and capture historical trends that influence future outputs. While LSTMs require more computational resources and training time, they often yield better performance on tasks involving time series data, such as wind power simulating based on climate variables.

To further enhance the temporal modeling capabilities, we include a Transformer-enhanced LSTM model. The Transformer component is integrated to focus attention on significant past events in the time series, selectively weighting them based on relevance to current predictions. This hybrid approach combines the sequential memory strength of LSTMs with the attention mechanisms of Transformers, allowing for dynamic weighting of historical patterns over varying time scales. This architecture is expected to improve forecast accuracy, especially in cases where specific climate conditions have a disproportionate impact on wind power production.

In Figure 8, we illustrate the MLP-based DNN architecture for wind power

prediction, showcasing the structure of the model, the input climate features, and the training process. By analyzing the performance of MLP, LSTM, and Transformer-enhanced LSTM models, we can assess the trade-offs between model complexity, computational cost, and predictive accuracy. This comparison provides insights into the optimal architecture for wind power simulating using processed CMIP climate datasets, helping to determine the most effective approach for leveraging both static and temporal features in climate-driven prediction tasks.

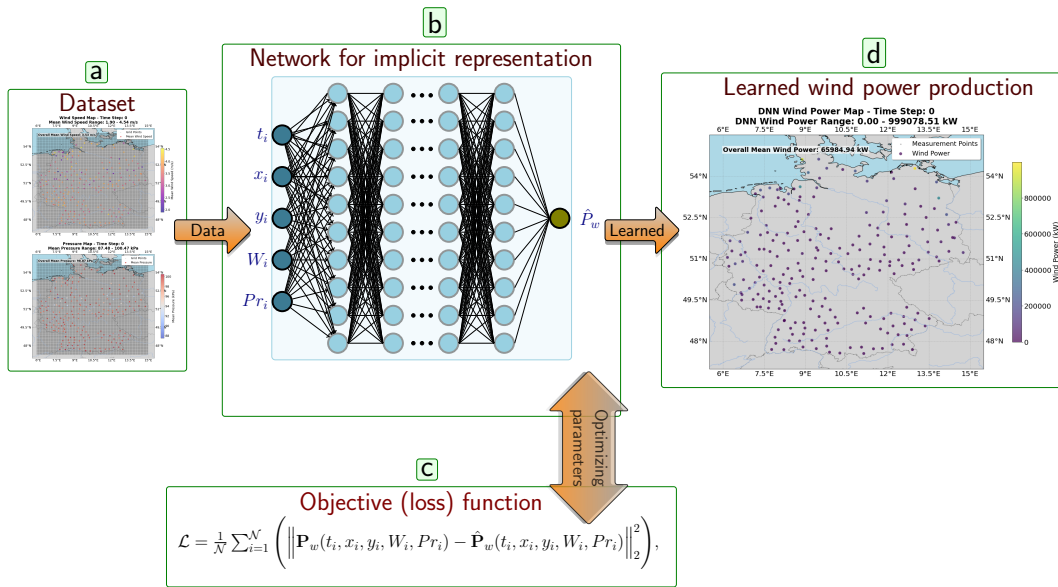


Figure 8: Deep learning architecture for wind power simulation. (a) climate dataset including wind speed and pressure surface; (b) MLP based DNN architecture takes 5 inputs, time t , x and y coordinates, wind speed W and pressure surface Pr ; (c) training of the DNN based on the mean square loss function; (d) learned wind power production.

In contrast, LSTM-DNNs are specifically designed to manage sequential data, making them highly effective for tasks where time series analysis is crucial. The unique architecture of LSTMs, with memory cells and gating mechanisms, allows them to retain information over long periods and capture dependencies that are spread out across time. This ability makes LSTMs particularly suited for scenarios where past climate conditions impact current or future wind power outputs. While LSTM-DNNs tend to have higher computational costs and require more time to train compared to MLPs, they often offer superior performance in forecasting tasks that involve sequential

or time-dependent data.

By comparing these architectures, we can better understand which model offers improved predictive capabilities when applied to processed CMIP climate datasets for wind power simulating, considering the trade-off between model complexity, training time, and accuracy.

Unlike MLP-DNNs, LSTM-DNN requires more sophisticated dataset preparation, therefore in the next subsection we provide its associated details.

5.1. Data Preparation Process for LSTM-Based Time Series wind power simulation

Preparing data for LSTM-based deep learning models is essential for capturing temporal dependencies in time series forecasting. This process involves four key stages: partitioning the dataset, generating sequences, reshaping the data, and initializing data loaders. Each stage ensures that the model receives well-structured inputs, enabling it to learn from historical data and generalize effectively to new, unseen data.

The first stage is to divide the dataset into training and testing subsets based on a predefined ratio of test data. This split is carried out chronologically to maintain the sequential nature of the data and avoid potential data leakage between the training and testing phases. This step is critical for ensuring that the model is evaluated on data that it has not seen during training, which is necessary for obtaining an unbiased assessment of its predictive performance.

Next, fixed-length sequences are created from the training and testing datasets. These sequences consist of consecutive data points over a specified length, providing the LSTM model with historical context that is crucial for making accurate predictions of future time steps. A rolling window approach is employed, extracting sequences of data followed by the corresponding target value for prediction.

Once the sequences are generated, they must be reshaped into the appropriate format for LSTM input, typically **Batch size**, **Sequence Length**, **number of features**. This reshaping step ensures that the data is compatible with the LSTM architecture, enabling efficient computation and facilitating parallel processing during model training.

Finally, data loaders are employed to manage the input data during training. By enabling mini-batch processing, data loaders improve computational efficiency, particularly when training on GPUs, and help accelerate the convergence of the model. Additionally, shuffling within batches promotes better

generalization, reducing the risk of overfitting and improving the model’s ability to make reliable predictions on unseen data.

algorithm 3 summarizes this data preparation process, providing a structured approach for training LSTM-based models in the context of wind power simulation.

5.2. Hardware setup

The training of our deep learning models was conducted on high-performance hardware to handle the computational demands of wind power simulation. Specifically, we utilized a single NVIDIA A100 GPU, equipped with 80 GB of Video Random Access Memory (VRAM)⁸, optimized for intensive machine learning tasks. This configuration included a memory allocation of 256 GB per CPU core to support large-scale data processing. The training job is managed through Simple Linux Utility for Resource Management (SLURM), using job-specific constraints to ensure compatibility with the A100 GPU’s extensive memory capacity, essential for efficient parallel processing and model training stability⁹. This advanced hardware setup enabled effective training of our models, enhancing both speed and accuracy in handling the complex temporal dependencies within the wind power data.

5.3. Code and data availability statement.

The CADNN model is implemented using the PyTorch framework, taking advantage of its advanced tools for constructing and training deep learning models. CADNN is openly available to enable reproducibility and facilitate further research in wind power simulation, leveraging climate datasets and DNNs for accurate, climate-informed predictions at this github repository¹⁰. The code for data extraction, interpolation, statistical analysis, visualization, DNN training and evaluation is provided in the associated repository.

⁸VRAM refers to the dedicated memory on a GPU used to store data that it needs to process and render tasks efficiently. Unlike standard RAM, which is used by the CPU, VRAM is optimized for handling high-speed operations related to graphics and parallel computations, such as deep learning, simulations, and large matrix operations.

⁹SLURM is a widely used open-source workload manager and job scheduling system for high-performance computing (HPC) environments. Originally developed by the Lawrence Livermore National Laboratory, SLURM manages and allocates resources such as CPUs, GPUs, and memory across computing nodes in an HPC cluster, allowing users to submit and schedule jobs efficiently.

¹⁰https://github.com/Ali-Forootani/neural_wind_model

Algorithm 3: Generalized Data Preparation for LSTM with Random Sampling

Input:

Data - Complete dataset with features and target values;
Coordinates - Optional spatial or feature coordinates;
Sequence Length - Desired length of input sequences for LSTM;
Test Data Size - Fraction of data to be used for testing;
Batch Size - Number of samples per batch in data loader;
Device - cuda if available, else cpu

Output:

Training sequences, Testing sequences, and their corresponding data loaders

1 **Set device based on GPU availability:**

2

device \leftarrow cuda if available, else cpu

3 **Step 1: Train-Test Split**

4 Partition Data into Train and Test subsets based on the specified Test Data Size, preserving the time order of samples.

5 **Step 2: Sequence Creation**

6 **for each data subset (*Train* and *Test*) do**

7 **for each time step i in data subset do**

8 Create a sequence from time step i to
 $i + \text{Sequence Length} - 1$

9 Assign the target value for each sequence as the value at
 $i + \text{Sequence Length}$ to align with next-step target

10 **Step 3: Sequence Reshaping for LSTM**

11 Reshape both Train and Test sequences to match the LSTM input format:

12 (Batch size, Sequence Length, number of features)

13 **Step 4: Data Loader Initialization**

14 **for each reshaped data subset (*Train* and *Test*) do**

15 Create a data loader with the specified Batch Size

16 Set shuffle to True for training and False for testing

17 **return** Training sequences, Testing sequences, and their corresponding data loaders

It includes detailed comments and instructions for reproducing the results. Additionally, a version will be archived on Zenodo¹¹ for reference.

5.4. DNN simulation setups

In this study, we explore three deep learning architectures to forecast wind power generation, comparing their abilities to model complex temporal patterns in time-series data. The first scenario employs a structured MLP model based on the Sinusoidal Representation Network (**SIREN**) architecture, designed for high-frequency signal representation Sitzmann et al. [56], Forootani and Benner [57], Forootani et al. [58]. This model leverages sinusoidal weight initialization to capture fine-grained temporal dependencies. The second scenario implements a **LSTM** network, a recurrent architecture that excels at learning sequential data patterns over long periods. In the third scenario, the deep learning model integrates both **LSTM** and **Transformer** layers, allowing it to leverage temporal dependencies and self-attention for modeling long-range dependencies. While all models share the same input and output configurations—an input of 5 features and a single-output prediction—each architecture is uniquely tailored to address the challenges of time-series forecasting. By comparing the **SIREN**-based MLP, **LSTM**, and **Transformer**-enhanced **LSTM** approaches, we aim to identify the most effective structure for capturing wind power patterns, optimizing both forecasting accuracy and training stability. Algorithm 4 summarizes the main training loop of the DNN structure considered in this article. In addition, out of total number of 679296 samples (as mentioned earlier 2928×232), 90% is randomly chosen for training the DNN structures and remaining 10% for testing the results.

MLP based CADNN. In the first scenario, we implement an MLP type DNN model using a structured, layered architecture tailored for wind power simulation. Our model configuration includes an input size of 5 features and a single-output prediction, passing through a sequence of six hidden layers, each with 128 hidden units. The model’s core is built around the **SIREN** (Sinusoidal Representation Network) architecture Sitzmann et al. [56], Forootani et al. [58], Forootani and Benner [57], Forootani et al. [59], known for its ability to represent high-frequency signals, making it particularly effective for

¹¹https://zenodo.org/account/settings/github/repository/Ali-Forootani/neural_wind_model, DOI: 10.5281/zenodo.14281375

time-series data in wind forecasting. The network architecture initializes the model parameters with a specific sinusoidal weight initialization method, which allows the model to capture fine-grained temporal patterns. Number of epochs is considered 30000 with learning rate $1e^{-5}$. Optimization is performed using the Adam optimizer with a weight decay of 1×10^{-6} to prevent overfitting. Additionally, we employ a Cyclic Learning Rate (CLR) scheduler in exponential range mode, which oscillates the learning rate between a base and maximum value, enhancing convergence by adjusting the learning rate dynamically. This architecture, optimized for periodic data, allows the model to leverage temporal dependencies effectively, providing a robust foundation for forecasting applications in renewable energy systems.

The scatter plot in fig. 9 illustrates the correlation between the true and predicted values generated by the MLP-DNN model for wind power simulation. Points closely aligned along the diagonal line indicate strong prediction accuracy, as the predicted values closely match the true values. It reveals a significant disparity between the predicted and true values, indicating that the MLP-DNN struggles to accurately forecast wind power. Many predictions deviate considerably from the expected values, suggesting potential shortcomings in the model’s ability to capture the underlying patterns in the data.

The histogram of prediction errors in fig. 9 presents the distribution of prediction discrepancies, defined as the difference between true and predicted values. A narrow centered distribution around zero with minimal spread indicates accurate predictions. The histogram of prediction errors further illustrates the model’s limitations, as it shows a wide spread of errors rather than clustering around zero. This indicates that the MLP-DNN frequently makes large errors in its predictions, highlighting the need for model refinement or alternative approaches to improve forecasting accuracy.

The plot fig. 10 illustrates the discrepancy between measured wind power generation and the MLP-DNN model’s predictions over the selected sample interval, indicating that the model struggles to accurately capture the variations in wind power output over the selected sample interval.

LSTM based CADNN. In the second scenario the deep learning architecture employed in our study consists of a LSTM network tailored for time-series forecasting. Specifically, the model is constructed with an input size of 5 features, passing sequentially through 6 stacked LSTM layers, each containing 128 hidden units. Each LSTM layer is initialized using Xavier initialization

to optimize weight distribution. Following the LSTM layers, a fully connected layer maps the output of the final LSTM layer to a single prediction, as defined by the output size of one. This architecture captures complex temporal dependencies in the data across multiple layers, enhancing its ability to model long-range patterns. We use the Adam optimizer with a learning rate scheduler that dynamically reduces the learning rate based on validation loss, ensuring stability in training and adaptability to diminishing gradients over time. Number of epochs is considered 30000 with initial learning rate $1e^{-3}$. This LSTM-based deep model is well-suited for our wind power simulation task due to its capacity to learn sequential dependencies and generate accurate time-step predictions.

The scatter plot in fig. 11 demonstrates a strong correlation between the true values and the predicted values, with most predictions closely aligning along the diagonal line, indicating that the LSTM-DNN model performs exceptionally well in accurately forecasting outcomes.

The histogram of prediction in fig. 11 errors reveals a tight distribution centered around zero, suggesting that the LSTM-DNN model consistently produces accurate predictions, with only a few instances of significant deviation, further highlighting its effectiveness in the task at hand.

The line plots in fig. 12 and fig. 13 vividly illustrate the performance of the LSTM-DNN model in predicting wind power generation, with the predicted values closely following the trend of the measured wind power, especially within the selected sample range. This indicates a strong predictive capability of the model, as evidenced by the minimal divergence between the predicted and true values.

LSTM-Transformer based CADNN. In this scenario, the deep learning architecture employed for time-series forecasting integrates both LSTM and Transformer layers. Specifically, the model is designed with an input size of 5 features, and it passes through 6 stacked LSTM layers, each containing 64 hidden units. The LSTM layers are initialized using Xavier initialization to ensure effective weight distribution. Following the LSTM layers, the output is passed through 2 Transformer layers, each utilizing 4 attention heads and a feed-forward network of size 20. This hybrid architecture enables the model to leverage both the temporal dependencies captured by the LSTM layers and the self-attention mechanism provided by the Transformer layers, improving its ability to model complex sequential patterns with long-range dependencies. The final output is generated by a fully connected layer that maps the output

of the last **Transformer** layer to a single prediction, as defined by the output size of one. The Adam optimizer is used with an initial learning rate of $1e^{-3}$, and a learning rate scheduler is applied to reduce the learning rate dynamically based on validation loss, ensuring training stability and adaptability. The model is trained for 30000 epochs, making it particularly well-suited for forecasting tasks that involve both short-term and long-term temporal dependencies, such as wind power simulation.

The scatter plot in fig. 14 illustrates a weak correlation between the true values and predicted values, with the majority of predictions clustering not closely along the diagonal line. This alignment indicates that the **LSTM-Transformer-DNN** model achieves low accuracy in forecasting wind power outputs.

Additionally, the histogram of prediction errors in fig. 14 shows a less concentrated distribution around zero, implying that the model consistently cannot provide precise predictions, with maximal occurrences of substantial error. This performance underscores the effectiveness of the **LSTM-Transformer-DNN** architecture for accurate time-series forecasting in wind power applications.

The plots in fig. 15, fig. 16, and fig. 17 highlight discrepancies between the measured wind power generation and the **LSTM-Transformer-DNN** model’s predictions over the selected sample interval. These inconsistencies suggest that the model struggles to capture the full extent of variability in wind power output.

6. Conclusion

This study made several important contributions to the literature on renewable energy forecasting by integrating large-scale CMIP6 climate data with advanced machine learning models for wind power prediction. We proposed a novel data processing pipeline that included temporal resampling, spatial interpolation, and normalization techniques, establishing best practices for adapting climate datasets for machine learning frameworks. Our comparative analysis of deep learning models demonstrated that LSTM networks were highly effective for this application, significantly outperforming MLPs and **Transformer**-enhanced LSTM models in capturing the temporal dependencies essential for accurate forecasts.

In addition, we provided a dedicated **Python** package built with **PyTorch** to support the reproducibility of our framework. This package offered mod-

Algorithm 4: General Training Loop for Deep Learning Model

Input: DNN Model \mathcal{M} , Optimizer \mathcal{O} (e.g., Adam optimizer),
Learning rate scheduler `scheduler`, Loss function \mathcal{L} ,
Number of epochs E , Training dataset loader \mathcal{D}_{train}

Output: Trained model parameters θ^* , total loss over epochs \mathcal{L}_{total}

```
1 Initialize empty list  $\mathcal{L}_{total} \leftarrow []$  // To store total losses
2 for epoch  $e \leftarrow 1$  to  $E$  do
3      $loss_{data} \leftarrow 0$ ;
4      $t_{start} \leftarrow \text{time.time}()$  // Record start time
5      $loss_{data} \leftarrow \mathcal{L}(\mathcal{D}_{train}, \mathcal{M})$  // Evaluate loss on train data
        using the model
6      $\mathcal{L} \leftarrow loss_{data}$  // Compute the total loss
7      $\mathcal{L}_{total}.\text{append}(\mathcal{L})$  // Store total loss
8     Gradient Calculation: ;
9      $\mathcal{O}.\text{zero\_grad}()$  // Zero the gradients
10     $\mathcal{L}.\text{backward}()$  // Backpropagation step
11     $\mathcal{O}.\text{step}()$  // Update model parameters
12    Learning Rate Scheduler: ;
13     $\text{scheduler}.\text{step}()$  // Adjust the learning rate
14    Logging (Optional): ;
15    Output current progress: epoch  $e$  and loss  $\mathcal{L}$ 
16 return  $\theta^*, \mathcal{L}_{total}$  // Return trained model parameters and
    total loss over epochs
```

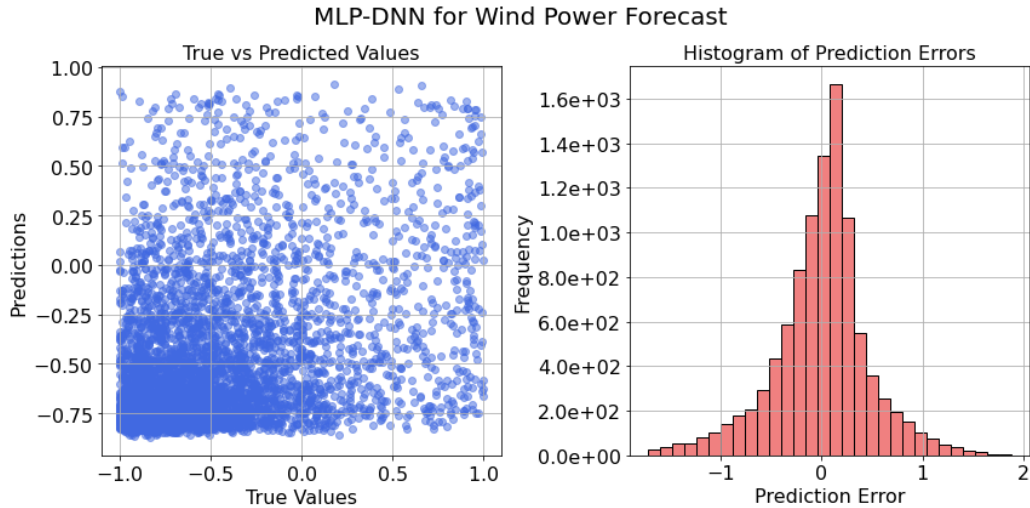


Figure 9: Prediction errors versus ground truth values in MLP-DNN.

ules for data preparation, model training, and evaluation, making it a practical resource for researchers and practitioners aiming to implement climate-based renewable energy forecasting models. By making this tool available, we fostered further research and application in this domain, supporting scalable and efficient forecasting methods.

This work advanced the field by providing a rigorous, adaptable framework that combined climate science with machine learning, addressing a critical need in renewable energy forecasting. The methodology and tools presented here not only enhanced wind power prediction accuracy but also laid the foundation for future innovations in climate data utilization for sustainable energy applications.

Acknowledgment

This study is funded by the *Man0EUvRE* (100695543), which is co-financed by means of taxation based on the budget adopted by the representatives of the Landtag of Saxony. “Man0EUvRE – Energy System Modelling for Transition to a net-Zero 2050 for EU via REPowerEU,” is funded by CETPartnership, the European Partnership under Joint Call 2022 for research proposals, co-funded by the European Commission (GA N°101069750).

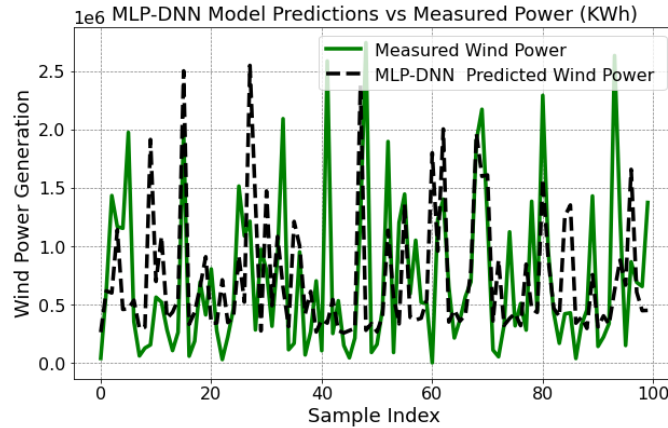


Figure 10: Comparing MLP based DNN versus true measurements for wind power simulation. It is worth to highlight that the true measurement model came from Lehneis and Thrän [60].

References

- [1] S. Oberthür, Hard or soft governance? the eu’s climate and energy policy framework for 2030, *Politics and Governance* 7 (2019) 17–27.
- [2] S. Asiaban, N. Kayedpour, A. E. Samani, D. Bozalakov, J. D. De Kooning, G. Crevecoeur, L. Vandeveldel, Wind and solar intermittency and the associated integration challenges: A comprehensive review including the status in the belgian power system, *Energies* 14 (2021) 2630.
- [3] L. Zhang, W. Song, E. Sun, Q. Zhang, D. Wu, F. Chen, Y. Liu, A high-altitude wind resource assessment method for decentralized wind power based on improved linear regression, *Renewable Energy* (2024) 121968.
- [4] D. Carvalho, A. Rocha, M. Gómez-Gesteira, C. S. Santos, Potential impacts of climate change on european wind energy resource under the cimp5 future climate projections, *Renewable Energy* 101 (2017) 29–40.
- [5] D. Carvalho, A. Rocha, M. Gómez-Gesteira, Ocean surface wind simulation forced by different reanalyses: Comparison with observed data along the iberian peninsula coast, *Ocean Modelling* 56 (2012) 31–42.

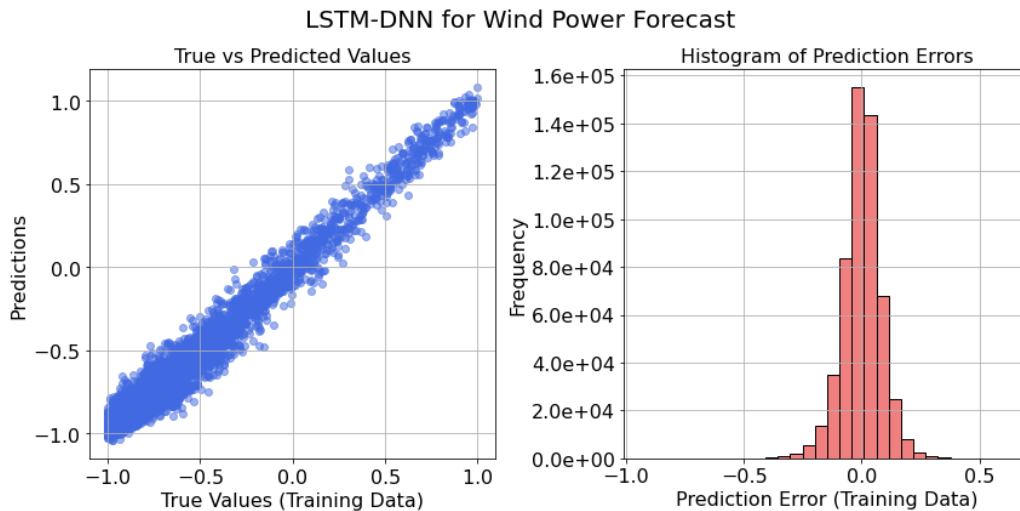


Figure 11: Prediction errors versus ground truth values in LSTM-DNN.

- [6] S. C. Pryor, R. J. Barthelmie, Climate change impacts on wind energy: A review, *Renewable and sustainable energy reviews* 14 (2010) 430–437.
- [7] A. Ahmadalipour, A. Rana, H. Moradkhani, A. Sharma, Multi-criteria evaluation of cmip5 gcms for climate change impact analysis, *Theoretical and applied climatology* 128 (2017) 71–87.
- [8] V. Eyring, S. Bony, G. A. Meehl, C. A. Senior, B. Stevens, R. J. Stouffer, K. E. Taylor, Overview of the coupled model intercomparison project phase 6 (cmip6) experimental design and organization, *Geoscientific Model Development* 9 (2016) 1937–1958.
- [9] T. Lovato, D. Peano, M. Butenschön, S. Materia, D. Iovino, E. Scocimarro, P. Fogli, A. Cherchi, A. Bellucci, S. Gualdi, et al., C mip6 simulations with the cmcc earth system model (cmcc-esm2), *Journal of Advances in Modeling Earth Systems* 14 (2022) e2021MS002814.
- [10] M. Reyers, J. Moemken, J. G. Pinto, Future changes of wind energy potentials over europe in a large cmip5 multi-model ensemble., *International Journal of Climatology* 36 (2016).
- [11] M. deCastro, X. Costoya, S. Salvador, D. Carvalho, M. Gómez-Gesteira, F. J. Sanz-Larruga, L. Gimeno, An overview of offshore wind energy

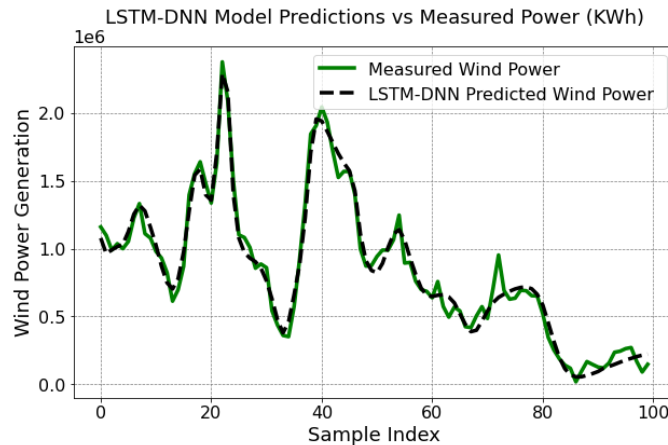


Figure 12: Comparing LSTM based DNN versus true measurements for wind power power simulation. It is worth to highlight that the true measurement model came from Lehneis and Thrän [60].

resources in europe under present and future climate, *Annals of the New York Academy of Sciences* 1436 (2019) 70–97.

- [12] F. Santos, M. Gómez-Gesteira, M. DeCastro, J. Añel, D. Carvalho, X. Costoya, J. Dias, On the accuracy of cordex rcms to project future winds over the iberian peninsula and surrounding ocean, *Applied Energy* 228 (2018) 289–300.
- [13] X. Costoya, A. Rocha, D. Carvalho, Using bias-correction to improve future projections of offshore wind energy resource: A case study on the iberian peninsula, *Applied Energy* 262 (2020) 114562.
- [14] L. Chen, Impacts of climate change on wind resources over north america based on na-cordex, *Renewable energy* 153 (2020) 1428–1438.
- [15] X. Costoya, M. DeCastro, D. Carvalho, M. Gómez-Gesteira, On the suitability of offshore wind energy resource in the united states of america for the 21st century, *Applied Energy* 262 (2020) 114537.
- [16] X. Costoya, M. DeCastro, D. Carvalho, Z. Feng, M. Gómez-Gesteira, Climate change impacts on the future offshore wind energy resource in china, *Renewable Energy* 175 (2021) 731–747.

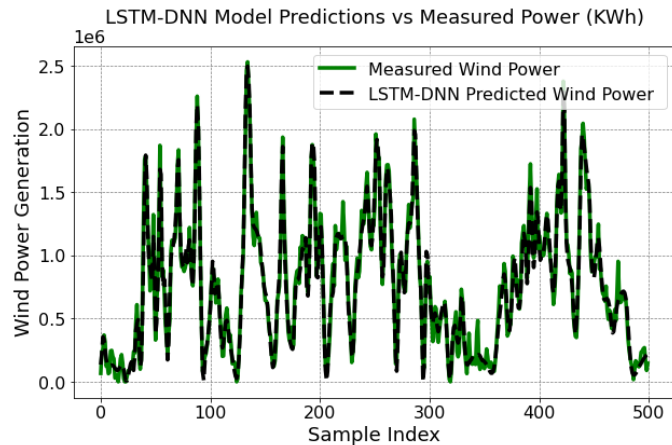


Figure 13: Comparing LSTM based DNN versus true measurements for wind power simulation. It is worth to highlight that the true measurement model came from Lehneis and Thrän [60].

- [17] A. A. Akinsanola, K. O. Ogunjobi, A. T. Abolude, S. Salack, Projected changes in wind speed and wind energy potential over west africa in cmip6 models, *Environmental Research Letters* 16 (2021) 044033.
- [18] N. Akhtar, B. Geyer, B. Rockel, P. S. Sommer, C. Schrum, Accelerating deployment of offshore wind energy alter wind climate and reduce future power generation potentials, *Scientific reports* 11 (2021) 11826.
- [19] P. M. Soares, D. C. Lima, A. Semedo, W. Cabos, D. V. Sein, Climate change impact on northwestern african offshore wind energy resources, *Environmental Research Letters* 14 (2019) 124065.
- [20] D. Carvalho, A. Rocha, X. Costoya, M. DeCastro, M. Gómez-Gesteira, Wind energy resource over europe under CMIP6 future climate projections: What changes from CMIP5 to CMIP6, *Renewable and Sustainable Energy Reviews* 151 (2021) 111594.
- [21] B. G. Brown, R. W. Katz, A. H. Murphy, Time series models to simulate and forecast wind speed and wind power, *Journal of Applied Meteorology and Climatology* 23 (1984) 1184–1195.
- [22] Y. Liu, J. Shi, Y. Yang, W.-J. Lee, Short-term wind-power prediction based on wavelet transform–support vector machine and statistic-

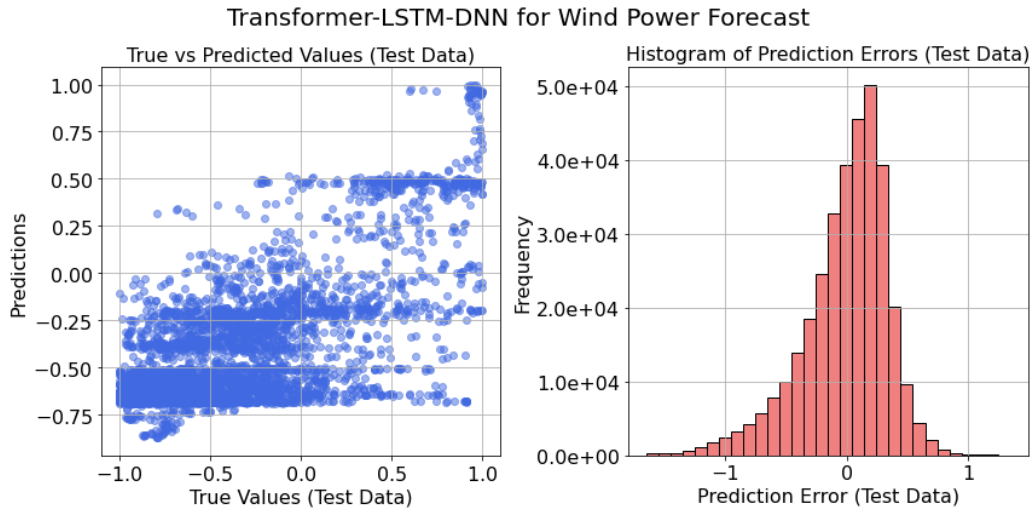


Figure 14: Prediction errors versus ground truth values in Transformer-based LSTM-DNN.

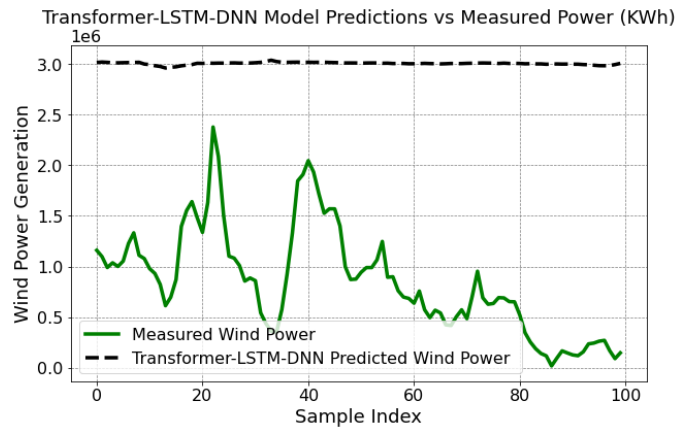


Figure 15: Comparing Transformer-LSTM based DNN versus true measurements for wind power production forecast

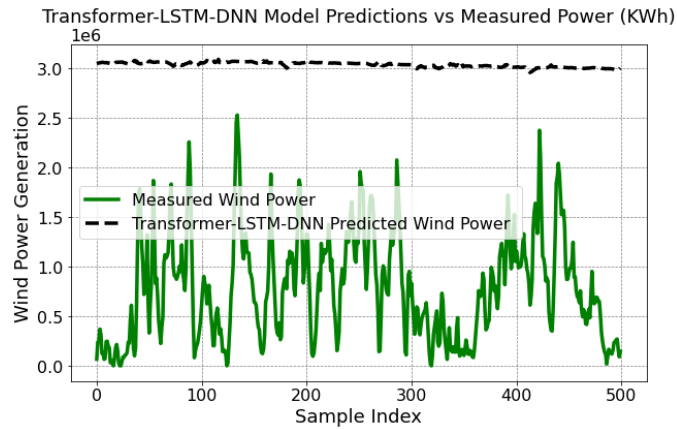


Figure 16: Comparing Transformer-LSTM based DNN versus true measurements for wind power simulation. It is worth to highlight that the true measurement model came from Lehneis and Thrän [60].

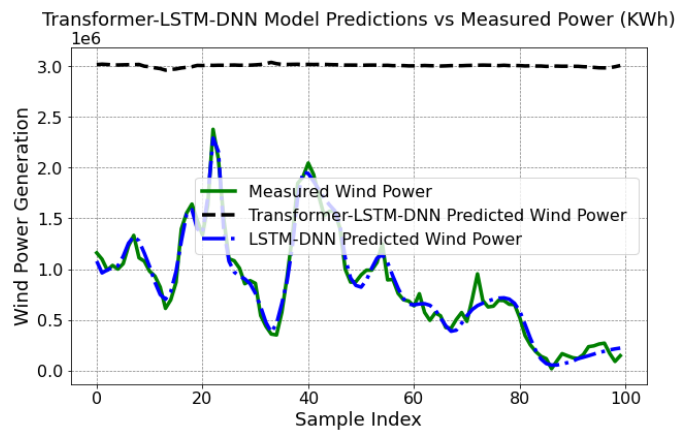


Figure 17: Comparing Transformer-LSTM based DNN versus true measurements and LSTMbased DNN for wind power simulation. It is worth to highlight that the true measurement model came from Lehneis and Thrän [60].

- characteristics analysis, *IEEE Transactions on Industry Applications* 48 (2012) 1136–1141.
- [23] X. Yuan, C. Chen, Y. Yuan, Y. Huang, Q. Tan, Short-term wind power prediction based on lssvm–gsa model, *Energy Conversion and Management* 101 (2015) 393–401.
- [24] D. Lee, R. Baldick, Short-term wind power ensemble prediction based on gaussian processes and neural networks, *IEEE Transactions on Smart Grid* 5 (2013) 501–510.
- [25] P. Pinson, H. A. Nielsen, H. Madsen, G. Kariniotakis, Skill forecasting from ensemble predictions of wind power, *Applied Energy* 86 (2009) 1326–1334.
- [26] M. G. De Giorgi, A. Ficarella, M. Tarantino, Error analysis of short term wind power prediction models, *Applied Energy* 88 (2011) 1298–1311.
- [27] K. Bhaskar, S. N. Singh, AWNN-assisted wind power forecasting using feed-forward neural network, *IEEE transactions on sustainable energy* 3 (2012) 306–315.
- [28] O. Abedinia, N. Amjady, Short-term wind power prediction based on hybrid neural network and chaotic shark smell optimization, *International journal of precision engineering and manufacturing-green technology* 2 (2015) 245–254.
- [29] M. C. Mabel, E. Fernandez, Analysis of wind power generation and prediction using ANN: A case study, *Renewable energy* 33 (2008) 986–992.
- [30] H. Chitsaz, N. Amjady, H. Zareipour, Wind power forecast using wavelet neural network trained by improved clonal selection algorithm, *Energy conversion and Management* 89 (2015) 588–598.
- [31] G. Grassi, P. Vecchio, Wind energy prediction using a two-hidden layer neural network, *Communications in Nonlinear Science and Numerical Simulation* 15 (2010) 2262–2266.
- [32] T. Hong, P. Pinson, S. Fan, Global energy forecasting competition 2012, 2014.

- [33] M. Lei, L. Shiyan, J. Chuanwen, L. Hongling, Z. Yan, A review on the forecasting of wind speed and generated power, *Renewable and sustainable energy reviews* 13 (2009) 915–920.
- [34] Y. Bao, H. Wang, B. Wang, Short-term wind power prediction using differential emd and relevance vector machine, *Neural Computing and Applications* 25 (2014) 283–289.
- [35] A. Costa, A. Crespo, J. Navarro, G. Lizcano, H. Madsen, E. Feitosa, A review on the young history of the wind power short-term prediction, *Renewable and Sustainable Energy Reviews* 12 (2008) 1725–1744.
- [36] A. M. Foley, P. G. Leahy, A. Marvuglia, E. J. McKeogh, Current methods and advances in forecasting of wind power generation, *Renewable energy* 37 (2012) 1–8.
- [37] A. Tascikaraoglu, M. Uzunoglu, A review of combined approaches for prediction of short-term wind speed and power, *Renewable and Sustainable Energy Reviews* 34 (2014) 243–254.
- [38] H. Peng, F. Liu, X. Yang, A hybrid strategy of short term wind power prediction, *Renewable Energy* 50 (2013) 590–595.
- [39] P. Pinson, H. Madsen, H. A. Nielsen, G. Papaefthymiou, B. Klöckl, From probabilistic forecasts to statistical scenarios of short-term wind power production, *Wind Energy: An International Journal for Progress and Applications in Wind Power Conversion Technology* 12 (2009) 51–62.
- [40] H. A. Nielsen, H. Madsen, T. S. Nielsen, Using quantile regression to extend an existing wind power forecasting system with probabilistic forecasts, *Wind Energy: An International Journal for Progress and Applications in Wind Power Conversion Technology* 9 (2006) 95–108.
- [41] S. Salcedo-Sanz, A. M. Perez-Bellido, E. G. Ortiz-García, A. Portilla-Figueras, L. Prieto, F. Correoso, Accurate short-term wind speed prediction by exploiting diversity in input data using banks of artificial neural networks, *Neurocomputing* 72 (2009) 1336–1341.
- [42] A. Troncoso, S. Salcedo-Sanz, C. Casanova-Mateo, J. Riquelme, L. Prieto, Local models-based regression trees for very short-term wind speed prediction, *Renewable Energy* 81 (2015) 589–598.

- [43] E. G. Ortiz-García, S. Salcedo-Sanz, Á. M. Pérez-Bellido, J. Gascón-Moreno, J. A. Portilla-Figueras, L. Prieto, Short-term wind speed prediction in wind farms based on banks of support vector machines, *Wind Energy* 14 (2011) 193–207.
- [44] W. Zhang, J. Wang, J. Wang, Z. Zhao, M. Tian, Short-term wind speed forecasting based on a hybrid model, *Applied Soft Computing* 13 (2013) 3225–3233.
- [45] X. Ma, Y. Jin, Q. Dong, A generalized dynamic fuzzy neural network based on singular spectrum analysis optimized by brain storm optimization for short-term wind speed forecasting, *Applied Soft Computing* 54 (2017) 296–312.
- [46] J. Jung, R. P. Broadwater, Current status and future advances for wind speed and power forecasting, *Renewable and Sustainable Energy Reviews* 31 (2014) 762–777.
- [47] D. Esmaili Aliabadi, N. Wulff, R. Lehneis, M. Sadr, F. Reutter, M. Jordan, P. Lehmann, D. Thrän, Climate change may impair the transition to a fully renewable energy system, Available at SSRN 4960744 (????).
- [48] R. Lehneis, D. Manske, B. Schinkel, D. Thrän, Power generation from variable renewable energies (VRE), *Helmholtz Climate Initiative* (2022) 213–215.
- [49] A. Forootani, A. Yazdizadeh, A. Aliabadi, Fault detection of gas unit of gilan combined cycle power plant using neural network, in: *The 3rd Conference on Thermal Power Plants*, IEEE, 2011, pp. 1–5.
- [50] R. Huang, C. Wei, B. Wang, J. Yang, X. Xu, S. Wu, S. Huang, Well performance prediction based on long short-term memory (lstm) neural network, *Journal of Petroleum Science and Engineering* 208 (2022) 109686.
- [51] A. Vaswani, N. Shazeer, N. Parmar, J. Uszkoreit, L. Jones, A. N. Gomez, Ł. Kaiser, I. Polosukhin, Attention is all you need, *Advances in neural information processing systems* 30 (2017).

- [52] A. Forootani, D. E. Aliabadi, D. Thraen, Bio-eng-lmm ai assist chatbot: A comprehensive tool for research and education, arXiv preprint arXiv:2409.07110 (2024).
- [53] A. Weiser, S. E. Zarantonello, A note on piecewise linear and multilinear table interpolation in many dimensions, *Mathematics of Computation* 50 (1988) 189–196.
- [54] M. R. Grose, S. Narsey, R. Trancoso, C. Mackallah, F. Delage, A. Dowdy, G. Di Virgilio, I. Watterson, P. Dobrohotoff, H. A. Rashid, et al., A cmip6-based multi-model downscaling ensemble to underpin climate change services in australia, *Climate Services* 30 (2023) 100368.
- [55] P. Virtanen, R. Gommers, T. E. Oliphant, M. Haberland, T. Reddy, D. Cournapeau, E. Burovski, P. Peterson, W. Weckesser, J. Bright, et al., *Scipy 1.0: fundamental algorithms for scientific computing in python*, *Nature methods* 17 (2020) 261–272.
- [56] V. Sitzmann, J. Martel, A. Bergman, D. Lindell, G. Wetzstein, Implicit neural representations with periodic activation functions, *Advances in neural information processing systems* 33 (2020) 7462–7473.
- [57] A. Forootani, P. Benner, GN-SINDy: Greedy sampling neural network in sparse identification of nonlinear partial differential equations, arXiv preprint arXiv:2405.08613 (2024).
- [58] A. Forootani, P. Goyal, P. Benner, A robust sindy approach by combining neural networks and an integral form, arXiv preprint arXiv:2309.07193 (2023).
- [59] A. Forootani, H. Kapadia, S. Chellappa, P. Goyal, P. Benner, Gs-pinn: Greedy sampling for parameter estimation in partial differential equations, arXiv preprint arXiv:2405.08537 (2024).
- [60] R. Lehneis, D. Thrän, Temporally and spatially resolved simulation of the wind power generation in germany, *Energies* 16 (2023) 3239.